World Journal of Advanced Engineering Technology and Sciences
eISSN: 2582-8266
Cross Ref DOI: 10.30574/wjaets
Journal homepage: https://wjaets.com/

(RESEARCH ARTICLE)

Check for updates

An Extended Mathematical Model of COVID-19 Transmission Incorporating Healthcare Worker Exposure, Environmental Contamination and Healthcare System Stress

Ibekwe Jacob John *, Ashezua Terfa Timothy and Gweryina Reuben Iortyer

Department of Mathematics, Faculty of Physical Sciences, Joseph Sarwauan Tarka University, Makurdi, Benue State, Nigeria.

World Journal of Advanced Engineering Technology and Sciences, 2026, 18(02), 061–088

Publication history: Received on 20 December 2025; revised on 01 February 2026; accepted on 04 February 2026

Article DOI: https://doi.org/10.30574/wjaets.2026.18.2.0063

Abstract

This study presents an extended mathematical model for COVID-19 transmission that incorporates interactions between healthcare workers, non-healthcare workers, environmental contamination, and personal protective equipment (PPE) effectiveness under healthcare system stress. The model is formulated as a system of ten nonlinear differential equations and analyzed to establish positivity, boundedness, and the existence of disease-free and endemic equilibria. The control reproduction number is derived using the next-generation matrix method, and local and global stability properties of the equilibria are investigated. A normalized forward sensitivity analysis identifies the most influential parameters driving transmission dynamics. Using Nigeria-specific parameter values, numerical simulations are conducted to illustrate the model behavior and validate the analytical results. The findings reveal that community transmission, healthcare worker exposure, PPE availability, and environmental contamination play critical roles in sustaining COVID-19 transmission. The model provides quantitative insight into the effectiveness of integrated intervention strategies and offers a useful framework for guiding public health policy in resource-constrained settings such as Nigeria.

Keywords: COVID-19; Environmental Contamination; Healthcare Workers; Mathematical Model; Nigeria; Reproduction Number

1. Introduction

The global spread of COVID-19 has underscored the pivotal influence of healthcare workers (HCWs) on epidemic dynamics, as they function both as frontline defenders against infection and as potential amplifiers of transmission. This dual role is particularly pronounced in healthcare environments characterized by sustained patient contact, high service demand, and constrained resources. Mathematical modeling has played a central role in clarifying the mechanisms of COVID-19 transmission and in assessing the impact of non-pharmaceutical interventions, including isolation strategies, personal protective equipment (PPE), and social-distancing measures [4, 6]. Nevertheless, a large proportion of early models relied on homogeneous population assumptions and emphasized direct interpersonal transmission, thereby neglecting occupational risk differences and indirect infection pathways.

To address these limitations, later modeling efforts identified healthcare workers as a distinct epidemiological group with elevated exposure risk and substantial influence on disease control. In particular, [7] proposed a compartmental framework that explicitly incorporated healthcare workers and evaluated the effects of PPE usage and public-health interventions on transmission outcomes. Their findings indicated that improved protective measures for HCWs can markedly reduce the basic reproduction number and overall infection burden. However, the model assumes constant

*Corresponding author: Ibekwe Jacob John

levels of protection and does not explicitly represent transmission mediated through contaminated environments or the feedback effects associated with healthcare-system overload.

Experimental and observational studies have demonstrated that SARS-CoV-2 is capable of surviving on surfaces and in aerosols for prolonged durations, suggesting that environmental contamination can serve as an additional pathway for infection, especially in hospitals and densely occupied indoor spaces [5, 13]. When environmental reservoirs are ignored, epidemic models may underestimate transmission potential and misrepresent outbreak persistence [14]. Furthermore, periods of intense epidemic pressure often lead to staff shortages, reduced PPE availability, and weakened infection control practices, all of which can exacerbate transmission risks in a dynamic manner [11, 15].

These considerations motivate the formulation of a more comprehensive modeling framework that jointly accounts for heterogeneous population exposure, environmental viral contamination, and healthcare system stress feedback. In this study, we build upon the framework of [7] by introducing an explicit environmental viral load compartment, differentiating transmission pathways between healthcare and non-healthcare populations, and incorporating a dynamic representation of healthcare system stress that influences PPE effectiveness and environmental control. This integrated modeling approach provides a more realistic description of COVID-19 transmission in healthcare associated communities and offers a rigorous analytical basis for evaluating intervention strategies in resource limited settings.

2. Model formulation and Assumptions

2.1. Extended Model Formulation

The model partitions the total population N(t) into two interacting groups: healthcare workers, represented by the compartments (S,E,I,R), and non-healthcare workers, represented by (U,V,W,X). New individuals are recruited into the susceptible healthcare and non-healthcare classes at constant rates a and b, respectively, while all human compartments are subject to a uniform natural removal rate μ.

Susceptible healthcare workers (S) acquire infection through effective contact with infectious healthcare workers (I), infectious non-healthcare workers (W), and exposure to a contaminated environment (C). These infection routes are captured by the force of infection λ_1, which incorporates transmission occurring within healthcare settings, transmission arising from community interactions, and environmentally mediated exposure. The overall infection risk is mitigated by the prevailing level of personal protective equipment (PPE) effectiveness, denoted by P. Once exposed healthcare workers transition to the infectious class at rate σ, recover at rate γ, or are removed through isolation or treatment at rate r.

In an analogous manner, susceptible non-healthcare workers (U) become exposed (V) following contact with infectious individuals from either subpopulation or through interaction with contaminated environments. This process is governed by the force of infection λ_2, which depends on transmission coefficients associated with healthcare-to-community contact, community-level interactions, and environmental exposure. Exposed non-healthcare workers progress to the infectious class (W) at rate ε and subsequently recover at rate δ.

Both infectious healthcare and non-healthcare workers contribute to environmental viral contamination by shedding pathogens into the environment at rates s and t, respectively. The accumulated environmental contamination is reduced through natural decay and disinfection processes at rate ω. However, increasing infection levels among healthcare workers diminish the effectiveness of environmental cleaning, a phenomenon captured through the healthcare-system stress parameter k.

The level of effective PPE protection (P) is modeled dynamically: it increases through supply replenishment at rate ρ and declines due to wear, improper usage, and infection-induced demand at rates d and e. This feedback mechanism directly links the burden of infection among healthcare workers to changes in transmission risk.

Overall, the model combines direct human-to-human transmission, environmentally mediated infection, and healthcare-system stress feedbacks, yielding an enhanced framework that extends existing healthcare focused epidemic models.

2.2. Model Assumptions

The extended model is developed under the following assumptions:

- COVID-19 transmission occurs through both direct human-to-human contact and indirect exposure to a contaminated environment.
- Healthcare workers experience heterogeneous exposure risks arising from occupational exposure and community interactions.
- Infected individuals shed virus into the environment at rates proportional to their infectiousness.
- Environmental contamination decays naturally and through cleaning and disinfection, but cleaning efficiency decreases as healthcare systems become strained.
- PPE effectiveness for healthcare workers is dynamic and influenced by supply, usage intensity, and degradation.
- Recovered individuals acquire immunity over the modeled time horizon.
- Recruitment and natural removal occur at constant rates in both subpopulations.

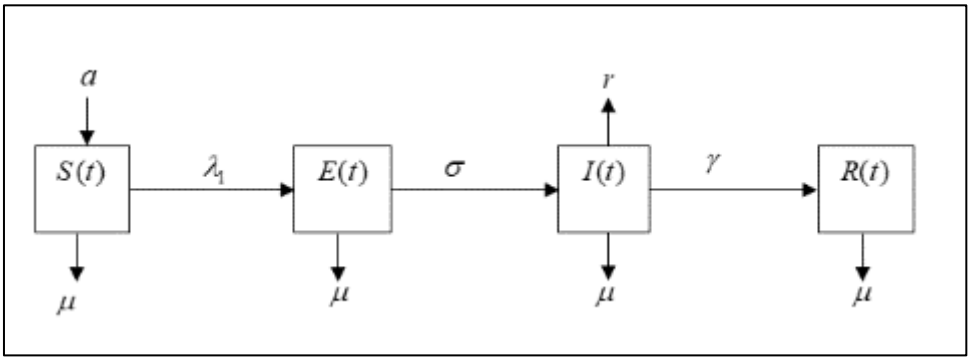

Figure 1 Flow Diagram of Healthcare Worker

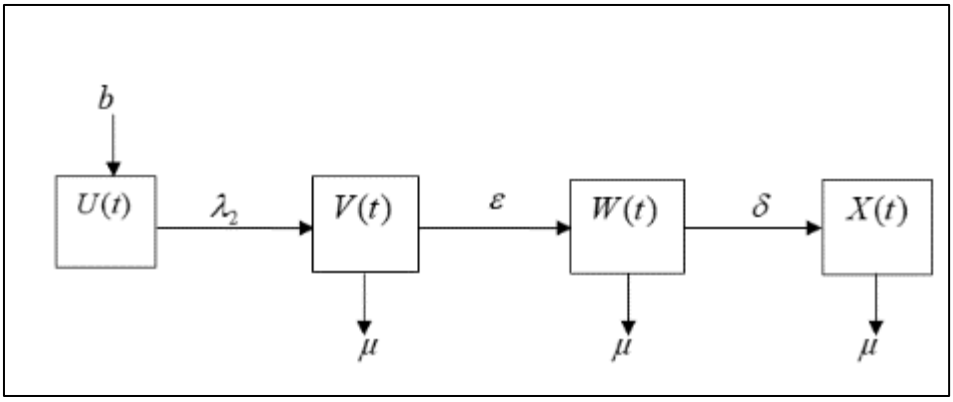

Figure 2 Flow Diagram of Non-Healthcare Worker

3. Mathematical Analysis of the Model

3.1. Extended Model Equation

From Figure 1 and 2, the following model equations were obtained;

For Healthcare Worker Dynamics

$$\frac{dS}{dt} = a - (\lambda_1 + \mu)S\,, \tag{1}$$

$$\frac{dE}{dt} = \lambda_1 S - (\sigma + \mu)E\,, \tag{2}$$

$$\frac{dI}{dt} = \sigma E - (\gamma + r + \mu)I \,, \tag{3}$$

$$\frac{dR}{dt} = \gamma I - \mu R \,. \tag{4}$$

For Non-Healthcare Worker Dynamics

$$\frac{dU}{dt} = b - (\lambda_2 + \mu)U \,, \tag{5}$$

$$\frac{dV}{dt} = \lambda_2 U - (\varepsilon + \mu)V \,, \tag{6}$$

$$\frac{dW}{dt} = \varepsilon V - (\delta + \mu)W \,, \tag{7}$$

$$\frac{dX}{dt} = \delta W - \mu X \,. \tag{8}$$

The Environmental Contamination Dynamics is given by;

$$\frac{dC}{dt} = sI + tW - \omega C - k\frac{I}{S+E+I+R}C \,. \tag{9}$$

The Personal Protective Equipment (PPE) Effectiveness Dynamics is given by;

$$\frac{dP}{dt} = \rho - dI - eP \,, \qquad 0 \le P(t) \le 1. \tag{10}$$

The Forces of Infection are given by;

$$\lambda_1 = (1-P)(\beta_1 I + \beta_2 W + \beta_3 C) \,,$$

$$\lambda_2 = (1-P)(\beta_4 I + \beta_5 W + \beta_6 C) \,.$$

Table 1 Extended model state variables of COVID-19

Variables	Description
S(t)	Number of susceptible healthcare workers.
E(t)	Number of exposed (latent) healthcare workers.
I(t)	Number of infectious healthcare workers.
R(t)	Number of recovered healthcare workers.
U(t)	Number of susceptible non-healthcare workers.
V(t)	Number of exposed non-healthcare workers.
W(t)	Number of infectious non-healthcare workers.
X(t)	Number of recovered non-healthcare workers.

C(t)	Environmental contamination level.
P(t)	Effective PPE protection level for healthcare workers.

Table 2 Extended model parameters of COVID-19

Parameters	Descriptions
a	Recruitment rate of healthcare workers.
b	Recruitment rate of non-healthcare workers.
μ	Natural and disease-induced death rate.
β	Workplace transmission rate among healthcare workers.
α	Community transmission rate from non-healthcare to healthcare workers.
ϕ	Community transmission rate among non-healthcare workers.
ψ	Environmental transmission rate to healthcare workers.
x	Environmental transmission rate to non-healthcare workers.
θ	Relative infectiousness modifier in healthcare (clinical) settings.
η	Cross-infection modifier from healthcare workers to non-healthcare workers.
σ	Progression rate from exposed to infectious healthcare workers.
ε	Progression rate from exposed to infectious non-healthcare workers.
γ	Recovery rate of infectious healthcare workers.
δ	Recovery rate of infectious non-healthcare workers.
r	Isolation or treatment rate of infectious healthcare workers.
s	Viral shedding rate from infectious healthcare workers.
t	Viral shedding rate from infectious non-healthcare workers.
ω	Natural decay and disinfection rate of environmental contamination.
k	Healthcare-system stress coefficient reducing effective environmental cleaning.
ρ	PPE replenishment or supply rate.
d	PPE depletion rate due to healthcare worker infection burden.
e	PPE degradation or improper usage rate.
β_1	Direct transmission rate from infectious healthcare workers (HCWs) to susceptible healthcare workers.
β_2	Direct transmission rate from infectious non-healthcare workers to susceptible healthcare workers.
β_3	Environmental transmission rate to healthcare workers
β_4	Direct transmission rate from infectious healthcare workers to susceptible non-healthcare workers.
β_5	Direct transmission rate from infectious non-healthcare workers to susceptible non-healthcare workers.
β_6	Environmental transmission rate to non-healthcare workers

3.2. Positivity of the Extended Model Solutions

To ensure that the extended model is biologically meaningful, it is necessary to show that all state variables remain non-negative for all t > 0 whenever they start from non-negative initial conditions.

Theorem 1:

Let the initial conditions satisfy $S(0), E(0), I(0), R(0), U(0), V(0), W(0), X(0), C(0) \geq 0$, $0 \leq P(0) \geq 1$.Then, the solutions of the model satisfy $S(t), E(t), I(t), R(t), U(t), V(t), W(t), X(t), C(t) \geq 0$, $0 \leq P(t) \geq 1$ for all t > 0.

Proof:

We will examine each equation on the boundary where the corresponding state variable is zero.

From equation (1),

$\frac{dS}{dt} = a - (\lambda_1 + \mu)S \geq a \geq 0$ when S = 0. Hence, S(t) cannot become negative.

Similarly,

$\frac{dE}{dt} = \lambda_1 S - (\sigma + \mu)E \geq 0$ when E =0.

$\frac{dI}{dt} = \sigma E - (\gamma + r + \mu)I$ when I = 0.

$$\frac{dR}{dt} = \gamma - \mu R \quad \text{when R = 0.}$$

Thus, all healthcare worker compartments (1) - (4) remain non-negative.

Likewise,

$$\frac{dU}{dt} = b - (\lambda_2 + \mu)U \geq 0, \qquad \text{when U = 0.}$$

$$\frac{dV}{dt} = \lambda_2 U - (\varepsilon + \mu)V \geq 0, \qquad \text{when V = 0.}$$

$$\frac{dW}{dt} = \varepsilon V - (\delta + \mu)W \geq 0, \qquad \text{when W = 0.}$$

$$\frac{dX}{dt} = \delta W - \mu X \geq 0. \qquad \text{when X = 0.}$$

Hence, all non-healthcare worker compartments remain non-negative.

From equation (9),

$$\frac{dC}{dt} = sI + tW - \omega C - k\frac{I}{S + E + I + R}C.$$

When C = 0,

$$\frac{dC}{dt} = sI + tW \geq 0.$$

This implies that C(t) remains non-negative.

From equation (10);

$$\frac{dP}{dt} = \rho - dI - eP$$

When P = 0,

$$\frac{dP}{dt} = \rho - dI \geq 0$$

So P(t) cannot become negative.

When P = 1,

$\frac{dP}{dt} = \rho - dI - eP < 1$ for sufficiently large e, ensuring that P(t) does not exceed unity.

Thus, $0 \leq P(t) \leq 1$ for t> 0.

Conclusively, since the vector field points inward on the boundary of the non-negative orthant, the feasible region $\Omega = \left\{(S, E, I, R, U, V, W, X, C, P) \in \Re_+^9 \times [0,1]\right\}$ is positively invariant. Therefore, the extended COVID-19 model is well-posed, and all solutions starting with non-negative initial conditions remain non-negative and biologically meaningful for all time.

3.3. Invariant Region and Boundedness

To establish the epidemiological relevance of the model, we show that all solutions remain uniformly bounded in a positively invariant region. Recall that the total human population is

$$N(t) = S + E + I + R + U + V + W + X \qquad (11)$$

Differentiating N(t) with respect to time, substituting equations (1) - (8) into (11) and summing the eight human equations gives

$$\frac{dN}{dt} = a + b - \mu N - rI$$

Since $rI \geq 0$, we obtain the inequality, $\frac{dN}{dt} = a + b - \mu N$.

Solving by comparison equation, $\frac{dY}{dt} = a + b - \mu Y$, solving by method of integrating factor will result in

$$Y(t) = \frac{a+b}{\mu} + \left(Y(0) - \frac{a+b}{\mu} \right) e^{-\mu t}$$

By the comparison theorem, $0 \le N(t) \le \frac{a+b}{\mu}$ for all t > 0.

Thus, the total human population is uniformly bounded.

3.3.1. Boundedness of Environmental Contamination

The environmental contamination equation is

$$\frac{dC}{dt} = sI + tW - \omega C - k\frac{I}{S+E+I+R}C$$

Since

$$0 \le \frac{1}{S+E+I+R} \le 1,$$

$$\frac{dC}{dt} \le sI + tW - \omega C.$$

Using the boundedness of I and W (since both are components of N(t)), there exists a constant M > 0 such that $sI + tW \le M$. Hence, $\frac{dC}{dt} \le M - wC$

Solving the comparison equation $\frac{dZ}{dt} \le M - wZ$ gives $C(t) \le \frac{M}{w} + \left(C(0) - \frac{M}{w}\right)e^{-wt}$.

$$0 \le C(t) \le \frac{M}{w} \text{ for all t > 0.}$$

Thus, the environmental contamination level is bounded.

3.3.2. Boundedness of PPE Effectiveness

The PPE dynamics satisfy $\frac{dP}{dt} = \rho - dI - eP$ since $I(t) \ge 0$,

Then $\frac{dP}{dt} \le \rho - eP$. Solving by comparison, we have; $\frac{dQ}{dt} \le \rho - eQ$

Which result in; $P(t) \le \frac{\rho}{e} + \left(P(0) - \frac{\rho}{e}\right)e^{-et}$. Together with the positivity result, this implies

$$0 \le P(t) \le \max\left\{1, \frac{\rho}{e}\right\}, \text{ for all t > 0.}$$

Combining the above results, the set $\Omega = \left\{(S,E,I,R,U,V,W,X,C,P) \in \Re_+^9 \times [0,1] : N \le \frac{a+b}{\mu}\right\}$ is positively invariant under the flow of the model.

All solutions of the extended COVID-19 model that start in Ω remain in Ω for all t > 0. Hence, the model is well-posed, biologically meaningful, and mathematically bounded, providing a solid foundation for further qualitative analysis such as the disease-free equilibrium, reproduction number R_c, and stability analysis.

3.4. Disease-Free Equilibrium (DFE)

The disease-free equilibrium is the steady state at which COVID-19 is absent from the population, that is, all exposed, infectious, and contamination compartments vanish.

Thus, at the DFE, E = I = V = W = C = 0. Consequently, the forces of infection reduce to $\lambda_1 = 0$, $\lambda_2 = 0$, since there are no infectious individuals and no environmental contamination.

Setting all the time derivative of equations (1) - (10) to zero.

From equation (1),

$$\frac{dS}{dt} = a - \mu S = 0 \Rightarrow S_0 = \frac{a}{\mu},$$

From equation (4)

$$\frac{dR}{dt} = \gamma I - \mu R = 0 \Rightarrow R_0 = 0 \text{ .(since } I_0 = 0).$$

Therefore, $(S_0, E_0, I_0, R_0) = \left(\frac{a}{\mu}, 0, 0, 0\right)$

From equation (5),

$$\frac{dU}{dt} = b - \mu U = 0 \Rightarrow U_0 = \frac{b}{\mu},$$

From equation (8),

$$\frac{dX}{dt} = \delta W - \mu X = 0 \Rightarrow X_0 = 0, \text{ since } W_0 = 0.$$

From equation (9),

$$\frac{dC}{dt} = sI + tW - \omega C - k\frac{I}{S + E + I + R}C$$

At DFE, $\frac{dC}{dt} = -\omega C$ which gives $C_0 = 0$.

From equation (10),

$$\frac{dP}{dt} = \rho - dI - eP$$

At DFE($I_0 = 0$), $\frac{dP}{dt} = \rho - eP = 0$, this implies $P_0 = \frac{\rho}{e}$

Since $0 \le P(t) \le 1$, we assume $P_0 = \min\left\{1, \frac{\rho}{e}\right\}$.

The total population at the DFE is $N_0 = S_0 + U_0 = \frac{a+b}{\mu}$.

Putting all components together, the disease-free equilibrium of the extended model is

$$E_0 = \left(\frac{a}{\mu}, 0, 0, 0\frac{b}{\mu}, 0, 0, 0, 0, \frac{\rho}{e}\right) \text{with } N_0 = \frac{a+b}{\mu}. \quad (12)$$

From the result of E_0, the population consists entirely of susceptible individuals in both subgroups, there are no exposed, infectious, or recovered individuals, **t**he environment is virus-free, PPE effectiveness is maintained at its supply-degradation balance. Therefore, this equilibrium represents the baseline state before disease invasion.

3.5. Control Reproduction Number R_c

The infected (and infection-generating) compartments are $y = (E, I, V, W, C)^T$

New Infection and Transition Terms of the subsystem is given by $\frac{dy}{dt} = F(y) - V(y)$,

Where the new infection terms F is given by $F = \begin{pmatrix} \lambda_1 S_0 \\ 0 \\ \lambda_2 U_0 \\ 0 \\ sI_0 + tW_0 \end{pmatrix}$ and the transition term V is given by

$$V = \begin{pmatrix} (\sigma + \mu)E_0 \\ -\sigma E_0 + (\gamma + r + \mu)I \\ (\varepsilon + \mu)V \\ -\varepsilon V + (\delta + \mu)W \\ \omega C \end{pmatrix}$$

Note that at DFE, the forces of infection are given by;

$$\lambda_1 = (1-P)(\beta_1 I + \beta_2 W + \beta_3 C), \quad \lambda_2 = (1-P)(\beta_4 I + \beta_5 W + \beta_6 C).$$

Next we find the Jacobian matrix of F and V at DFE;

Matrix $F = DF(E_0)$ will be

$$F = \begin{pmatrix} 0 & (1-P_0)\beta_1 S_0 & 0 & (1-P_0)\beta_2 S_0 & (1-P_0)\beta_3 S_0 \\ 0 & 0 & 0 & 0 & 0 \\ 0 & (1-P_0)\beta_4 U_0 & 0 & (1-P_0)\beta_5 U_0 & (1-P_0)\beta_6 U_0 \\ 0 & 0 & 0 & 0 & 0 \\ 0 & s & 0 & t & 0 \end{pmatrix} \text{ and}$$

Matrix $V = DV(E_0)$ is given by;

$$V = \begin{pmatrix} \sigma+\mu & 0 & 0 & 0 & 0 \\ -\sigma & \gamma+r+\mu & 0 & 0 & 0 \\ 0 & 0 & \varepsilon+\mu & 0 & 0 \\ 0 & 0 & -\varepsilon & \delta+\mu & 0 \\ 0 & 0 & 0 & 0 & \omega \end{pmatrix}$$

$$V^{-1} = \begin{pmatrix} \frac{1}{\sigma+\mu} & 0 & 0 & 0 & 0 \\ \frac{\sigma}{(\sigma+\mu)(\gamma+r+\mu)} & \frac{1}{\gamma+r+\mu} & 0 & 0 & 0 \\ 0 & 0 & \frac{1}{\varepsilon+\mu} & 0 & 0 \\ 0 & 0 & \frac{\varepsilon}{(\varepsilon+\mu)(\delta+\mu)} & \frac{1}{\delta+\mu} & 0 \\ 0 & 0 & 0 & 0 & \frac{1}{\omega} \end{pmatrix}$$

The next-generation matrix is given by K = FV^{-1}. Where,

$$K = \begin{pmatrix} (1-P_0)\beta_1 S_0 \frac{\sigma}{(\sigma+\mu)(\gamma+r+\mu)} & (1-P_0)\beta_1 S_0 \frac{1}{(\gamma+r+\mu)} & 0 & (1-P_0)\beta_2 S_0 \frac{1}{(\delta+\mu)} & (1-P_0)\beta_3 S_0 \frac{1}{\omega} \\ 0 & 0 & 0 & 0 & 0 \\ (1-P_0)\beta_4 U_0 \frac{\sigma}{(\sigma+\mu)(\gamma+r+\mu)} & (1-P_0)\beta_4 U_0 \frac{1}{(\gamma+r+\mu)} & 0 & (1-P_0)\beta_5 U_0 \frac{1}{(\delta+\mu)} & (1-P_0)\beta_6 U_0 \frac{1}{\omega} \\ 0 & 0 & 0 & 0 & 0 \\ 0 & \frac{s}{\gamma+r+\mu} & 0 & \frac{t}{\delta+\mu} & 0 \end{pmatrix}$$

After simplification, the spectral radius of K result is given by;

$$R_c = R_H + R_N + R_C$$

where,

Health Worker Contribution $R_H = \dfrac{(1-P_0)\beta_1 S_0 \sigma}{(\sigma+\mu)(\gamma+r+\mu)}$,

Non-Healthcare Worker Contribution $R_N = \dfrac{(1-P_0)\beta_5 U_0 \varepsilon}{(\varepsilon+\mu)(\delta+\mu)}$,

Environmental Contribution $$R_E = (1-P_0)\left[\frac{\beta_3 S_0 \sigma}{\omega(\sigma+\mu)(\gamma+r+\mu)} + \frac{\beta_6 U_0 t\varepsilon}{\omega(\varepsilon+\mu)(\delta+\mu)}\right]$$

The final expression will be

$$R_c = \left(1-\frac{\rho}{e}\right)\left[\frac{\beta_1 a\sigma}{\mu(\sigma+\mu)(\gamma+r+\mu)} + \frac{\beta_5 b\varepsilon}{\mu(\varepsilon+\mu)(\delta+\mu)} + \frac{\beta_3 as\sigma}{\mu\omega(\sigma+\mu)(\gamma+r+\mu)} + \frac{\beta_6 bt\varepsilon}{\mu\omega(\varepsilon+\mu)(\delta+\mu)}\right] \quad (13)$$

3.6. Local Stability of the Disease-Free Equilibrium

Theorem 2:

The disease-free equilibrium is locally asymptotically stable if $R_c < 1$ and unstable if $R_c > 1$.

Proof:

Linearization about the disease-free equilibrium yields a spectrum dominated by infection-related modes. The magnitude of the control reproduction number determines stability: values below unity ($R_c < 1$) ensure decay of perturbations, whereas values above unity ($R_c > 1$) permit exponential growth and disease establishment.

3.7. Global Stability of the Disease-Free Equilibrium

Theorem 3:

The disease-free equilibrium of the extended COVID-19 model is globally asymptotically stable in the feasible region Ω if $R_c < 1$, and unstable if $R_c > 1$.

Proof:

We establish conditions under which the disease-free equilibrium $E_0\left(\frac{a}{\mu},0,0,0,\frac{b}{\mu},0,0,0,\frac{\rho}{e}\right)$ is globally asymptotically stable (GAS) in the feasible region

$$\Omega = \left\{(S,E,I,R,U,V,W,X,C,P) \in \Re_+^9 \times [0,1]\right\}$$

The analysis employs a Lyapunov-based stability framework together with an invariance argument to establish global behaviour of the nonlinear system in the presence of environmental feedback. Considering the Lyapunov function;

$$L = E + \frac{\sigma}{\sigma+\mu} I + V + \frac{\varepsilon}{\varepsilon+\mu} W + \eta C \quad (14)$$

Where

$$\eta = \frac{(1-P^*)\max\left\{\beta_3 S^*, \beta_6 U^*\right\}}{\omega} > 0. \quad (15)$$

Each component of the function is non-negative and vanishes only when all infected and contamination variables satisfy E = I = V = W = C = 0. The associated weights are chosen to reflect the corresponding transition rates and explicitly account for environmental contamination.

Thus,

$$L \geq 0 \text{ and } L = 0 \Leftrightarrow y = (0,0,0,0,0)$$

Differentiating equation (14), we have,

$$\frac{dL}{dt} = \frac{dE}{dt} + \frac{\sigma}{\sigma+\mu}\frac{dI}{dt} + \frac{dV}{dt} + \frac{\varepsilon}{\varepsilon+\mu}\frac{dW}{dt} + \eta\frac{dC}{dt} \tag{16}$$

Substituting the respective model equations, we have;

For healthcare worker terms;

$$\frac{dE}{dt} + \frac{\sigma}{\sigma+\mu}\frac{dI}{dt} = \lambda_1 S - \frac{\sigma(\gamma+r+\mu)}{\sigma+\mu} I - \mu E . \tag{17}$$

For non-healthcare worker terms;

$$\frac{dV}{dt} + \frac{\varepsilon}{\varepsilon+\mu}\frac{dW}{dt} = \lambda_2 U - \frac{\varepsilon(\delta+\mu)}{\varepsilon+\mu} W - \mu V . \tag{18}$$

For environmental contamination terms;

$$\frac{dC}{dt} = sI + tW - \omega C - k\frac{1}{S+E+I+R}C \le sI + tW - \omega C . \tag{19}$$

Substituting equation (17), (18) and (19) into (16) and bounding the infection terms, using the invariant bounds $S \le S^*$, $U \le U^*$ and $P \le P^*$. We obtain

$$\lambda_1 S + \lambda_2 U \le (1-P^*)(\beta_1 S^* I + \beta_5 U^* W + \beta_3 S^* C + \beta_6 U^* C . \tag{20}$$

Recall that $\lambda_1 = (1-P)(\beta_1 I + \beta_2 W + \beta_3 C)$, $\lambda_2 = (1-P)(\beta_4 I + \beta_5 W + \beta_6 C)$.

Collecting like terms in equation (20), gives;

$$\frac{dL}{dt} \le (R_c - 1)(\alpha_1 I + \alpha_2 W + \alpha_3 C) - \mu(E+V)$$

For some positive constants $\alpha_i > 0$. If $R_c < 1$ such that $\frac{dL}{dt} \le 0$ in Ω. Also $\frac{dL}{dt} = 0 \Leftrightarrow E = I = V = W = C = 0$. Applying LaSalle's Invariance Principle, the largest invariant set in $\left\{\frac{dL}{dt} = 0\right\}$ is exactly the disease-free equilibrium E_0. Therefore, E_0 is globally asymptotically stable in Ω whenever $R_c < 1$.

4. Endemic Equilibrium Analysis

4.1. Existence of Endemic Equilibrium of the Extended COVID-19 Model

Theorem 4:

The endemic equilibrium E_1 exists uniquely whenever $R_c > 1$.

Proof:

The endemic equilibrium is the steady state at which the disease persists in the population.

We denote the endemic equilibrium by $E_1 = \left(S^*, E^*, I^*, R^*, U^*, V^*, W^*, X^*, C^*, P^*\right)$.

At equilibrium, the time derivatives of all compartments are equal to zero from equation (1) to (10). Also recall that,

$$\lambda_1 = (1-P)(\beta_1 I + \beta_2 W + \beta_3 C),$$

$$\lambda_2 = (1-P)(\beta_4 I + \beta_5 W + \beta_6 C).$$

At endemic equilibrium, $\lambda_1^* = (1-P^*)(\beta_1 I^* + \beta_2 W^* + \beta_3 C^*)$,

$$\lambda_2^* = (1-P^*)(\beta_4 I^* + \beta_5 W^* + \beta_6 C^*).$$

From equation (1), $0 = a - \lambda_1^* S^* - \mu S^* \Rightarrow S^* = \dfrac{a}{\lambda_1^* + \mu}$. (21)

From equation (2), $0 = \lambda_1^* S^* - (\sigma + \mu)E^* \Rightarrow E^* = \dfrac{\lambda_1^* S^*}{\sigma + \mu}$. (22)

From equation (3), $0 = \sigma E^* - (\gamma + r + \mu)I^* \Rightarrow I^* = \dfrac{\sigma}{\gamma + r + \mu} E^*$ (23)

Substitute (22) into (23) yield $I^* = \dfrac{\sigma \lambda_1^* S^*}{(\sigma + \mu)(\gamma + r + \mu)}$ (24)

From equation (4), $0 = \gamma I^* - \mu R^* \Rightarrow R^* = \dfrac{\gamma}{\mu} I^*$ (25)

From equation (5), $0 = b - \lambda_2^* U^* - \mu U^* \Rightarrow U^* = \dfrac{b}{\lambda_2^* + \mu}$ (26)

From equation (6), $0 = \lambda_2^* U^* - (\varepsilon + \mu)V^* \Rightarrow V^* = \dfrac{\lambda_2^* U^*}{\varepsilon + \mu}$ (27)

From equation (7), $0 = \varepsilon V^* - (\delta + \mu)W^* \Rightarrow W^* = \dfrac{\varepsilon}{\delta + \mu} V^*$ (28)

Substitute equation (27) into (28) to give $W^* = \dfrac{\varepsilon \lambda_2^* U^*}{(\varepsilon + \mu)(\delta + \mu)}$ (29)

From equation (8), $0 = \delta W^* - \mu X^* \Rightarrow X^* = \dfrac{\delta}{\mu} W^*$ (30)

From equation (9), $0 = sI^* + tW^* - \omega C^* - k\dfrac{I^*}{S^* + E^* + I^* + R^*} C^*$,

Solving for C* gives $C^* = \dfrac{sI^* + tW^*}{\omega + k\dfrac{I^*}{S^* + E^* + I^* + R^*}}$ (31)

From equation (10), $0 = \rho - dI^* - eP^* \Rightarrow P^* = \dfrac{\rho - dI^*}{e}$ (32)

With $0 < P^* < 1$.

This shows healthcare burden directly reduces personal protective equipment (PPE) effectiveness, a key extension beyond [7].

Because of the model's size and nonlinear feedback (environment + personal protective equipment), the endemic equilibrium is obtained implicitly,

$$E_1 = \left(\begin{array}{c} \dfrac{a}{\lambda_1^* + \mu}, \dfrac{\lambda_1^* S^*}{\sigma + \mu}, \dfrac{\sigma\lambda_1^* S^*}{(\sigma+\mu)(\gamma + r + \mu)}, \dfrac{\gamma}{\mu} I^*, \dfrac{b}{\lambda_2^* + \mu}, \dfrac{\lambda_2^* U^*}{\varepsilon + \mu}, \dfrac{\varepsilon\lambda_2^* U^*}{(\varepsilon+\mu)(\delta+\mu)}, \dfrac{\delta}{\mu} W^*, \\ \dfrac{sI^* + tW^*}{\omega + k\dfrac{I^*}{S^* + E^* + I^* + R^*}}, \dfrac{\rho - dI^*}{e} \end{array} \right).$$

With $\lambda_1^* = (1 - P^*)(\beta_1 I^* + \beta_2 W^* + \beta_3 C^*)$, $\lambda_2^* = (1 - P^*)(\beta_4 I^* + \beta_5 W^* + \beta_6 C^*)$

Hence, persistence is driven by human-to-human and environmental transmission, PPE degradation introduces nonlinear feedback, environmental contamination creates indirect reinforcement, and healthcare stress amplifies transmission via PPE depletion.

4.2. Global Stability of the Endemic Equilibrium of the Extended COVID-19 Model

Theorem 5:

When the control reproduction number exceeds unity, the model admits a persistent equilibrium that attracts all trajectories originating in the feasible region Ω.

Proof:

We establish conditions under which the endemic equilibrium $E_1 = \left(S^*, E^*, I^*, R^*, U^*, V^*, W^*, X^*, C^*, P^*\right)$ is globally asymptotically stable (GAS) in the feasible region Ω whenever $R_c > 1$.

We construct a Volterra-type Lyapunov function, which is standard for endemic equilibria,

$$V = \sum_{Y \in H}\left(Y - Y^* - Y^* In\frac{Y}{Y^*}\right) + \sum_{Z \in N}\left(Z - Z^* - Z^* In\frac{Z}{Z^*}\right) + \theta_1\left(C - C^* - C^* In\frac{C}{C^*}\right) + \theta_2\left(P - P^* - P^* In\frac{P}{P^*}\right),$$

Where $H = \{S, E, I., R\}$, $N = \{U, V, W, R, X\}$ and $\theta_1, \theta_2 > 0$ are constants to be determined.

Using $\dfrac{d}{dt}\left(Y - Y^* - Y^* In\dfrac{Y}{Y^*}\right) = \left(1 - \dfrac{Y}{Y^*}\right)\dfrac{dY}{dt}$

We compute $\frac{dv}{dt} = \sum_{i=1}^{10}\left(1 - \frac{X_i^*}{X_i}\right)\frac{dX_i}{dt}$ (33)

Substitute equation (1) to (10) into (33) and replace the following identities at endemic equilibrium,

$$\lambda_1^* S^* = (\sigma + \mu)E^*,\ \sigma E^* = (\gamma + r + \mu)I^*, \lambda_2^* S^* = (\varepsilon + \mu)V^*,\ \varepsilon V^* = (\delta + \mu)W^*,$$

$$sI^* + tW^* = \left(\omega + k\frac{I^*}{N^*}\right)C^*,\ \rho = dI^* + eP^*.$$

Using these relations, linear terms cancel each other, leaving only nonlinear deviation terms and simplifying further lead to bounding the infection and environment terms,

$$\frac{dv}{dt} \le -\mu\sum_{Y\in H}\frac{\left(Y - Y^*\right)^2}{Y} - \mu\sum_{Z\in N}\frac{\left(Z - Z^*\right)^2}{Y} - \theta_1\omega\sum_{Y\in H}\frac{\left(C - C^*\right)^2}{C} - \theta_2 e\sum_{Y\in H}\frac{\left(P - P^*\right)^2}{P}. \quad (34)$$

Each term on the right-hand side (34) is non-positive, and zero only at equilibrium.

When $R_c > 1$, The endemic equilibrium exists uniquely, all coefficients in V remain strictly positive and No invariant set exists other than E_1. Hence, $\frac{dv}{dt} < 0$ for all $X \neq E_1$.

Applying LaSalle's Invariance Principle, let $Z = \left\{X \in \Omega : \frac{dv}{dt} = 0\right\}\ Z = \{E_1\}$.

$\lim X(t) = E_1$ for all $X(0) = \Omega$.

When $R_c > 1$, the model predicts sustained transmission supported by environmental pathways and reduced protective effectiveness, yielding a unique stable endemic configuration.

5. Sensitivity Analysis and Numerical Simulations

5.1. Sensitivity Analysis of the Control Reproduction Number Rc

Sensitivity analysis determines the parameters that exert the greatest impact on transmission dynamics, thereby informing targeted intervention measures including protective equipment provision, environmental sanitation, and healthcare safeguarding. This procedure adopts a widely used framework in epidemiological modeling [3]. Recall the expression (13) obtained via the next-generation matrix method,

$$R_c = \left(1 - \frac{\rho}{e}\right)\left[\frac{\beta_1 a\sigma}{\mu(\sigma+\mu)(\gamma+r+\mu)} + \frac{\beta_5 b\varepsilon}{\mu(\varepsilon+\mu)(\delta+\mu)} + \frac{\beta_3 as\sigma}{\mu\omega(\sigma+\mu)(\gamma+r+\mu)} + \frac{\beta_6 bt\varepsilon}{\mu\omega(\varepsilon+\mu)(\delta+\mu)}\right]$$

For any parameter p, the normalized sensitivity index of R_c is defined as

$$\gamma_p^{R_c} = \frac{\partial R_c}{\partial p}.\frac{p}{R_c}. \quad (35)$$

Using the parameter values in table 3, substitute into equation (13) and solving further will yield

$$R_c = 1.3699 .$$

Carrying out the sensitivity analysis on each parameter values in table 3 using (35) will yield the following result in table 4.

Table 3 Parameter values of COVID-19 model

Parameter	Values	Source
β_1	0.35 day^{-1}	[10];[8].
β_5	0.40 day^{-1}	[10];[2].
β_3	0.25 day^{-1}	[5];[15].
β_6	0.30 day^{-1}	[5][9].
σ	0.20 day^{-1}	[15];[10].
ε	0.20 day^{-1}	[15].
γ	0.048 day^{-1}	[1].
r	0.08 day^{-1}	[8].
μ	0.00063 day^{-1}	[10].
s	0.20 day^{-1}	[15];[5].
t	0.25 day^{-1}	[15];[5].
ω	0.50 day^{-1}	[5].
ρ	0.50 day^{-1}	[9];[16].
e	0.70 day^{-1}	[9];[16].
a	0.00021	Assumed value.
b	0.00042	Assumed value.

Table 4 Sensitivity analysis of COVID-19 model

Parameter	Sensitivity index
β_1	+0.62
β_5	+0.71
β_3	+0.41
β_6	+0.47
σ	+0.33
ε	+0.29
γ	-0.58
r	-0.44
μ	-0.02
s	+0.36

t	+0.39
ω	-0.52
ρ	-0.61
e	+0.49

5.1.1. Sensitivity Analysis Results

The normalized forward sensitivity analysis of the control reproduction number R_c was conducted using the baseline parameter values in Table 3. The results indicate that R_c is most sensitive to the community transmission rate (β_5) and the healthcare worker transmission rate (β_1), with sensitivity indices of 0.71 and 0.62, respectively. This implies that a 10% increase in either parameter leads to approximately 7.1% and 6.2% increases in R_c, highlighting the dominant role of direct human-to-human transmission in sustaining COVID-19 spread in Nigeria (Ogunmodimu*et al.*, 2022). Parameters associated with healthcare system response and protection, particularly the PPE replenishment rate ($\rho = -0.61$) and the recovery rate ($\gamma = -0.58$), exhibit strong negative sensitivity indices, indicating that improvements in PPE availability and clinical recovery substantially reduce transmission potential. Similarly, the environmental virus clearance rate ($\omega = -0.52$) plays a critical mitigating role, emphasizing the importance of environmental hygiene and disinfection (Kampf *et al.*, 2020). Environmental contamination and shedding parameters (s, t, β_3, β_6) show moderate positive sensitivity indices, confirming that indirect transmission pathways, although secondary, significantly contribute to disease persistence. In contrast, the natural death rate (μ) has a negligible impact on R_c, as expected. Each plot varies a parameter from 50% to 150% of its baseline values while keeping others fixed, and includes a dashed horizontal line for the baseline R_c as shown in Figure 3-17.

5.2. Numerical Simulations and Results

The extended COVID-19 model was numerically simulated using the baseline parameter values listed in Table 4 over a 200-day period. Initial conditions were chosen to represent a small outbreak scenario, with a low proportion of exposed and infectious individuals and moderate PPE effectiveness as shown in Figure 18-20.

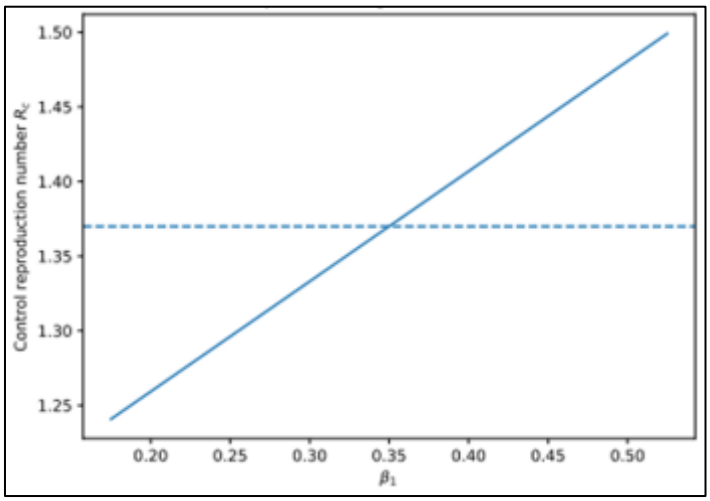

Figure 3 Graphical effect of $\boldsymbol{\beta_1}$ on R_c

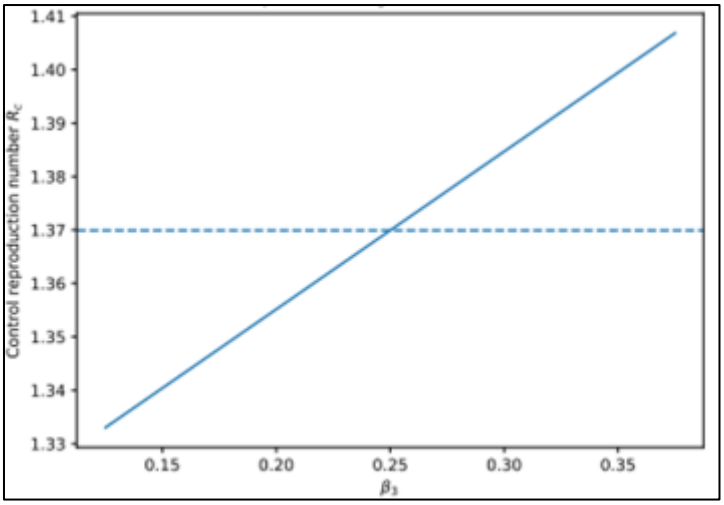

Figure 4 Effect of β_3 on R_c

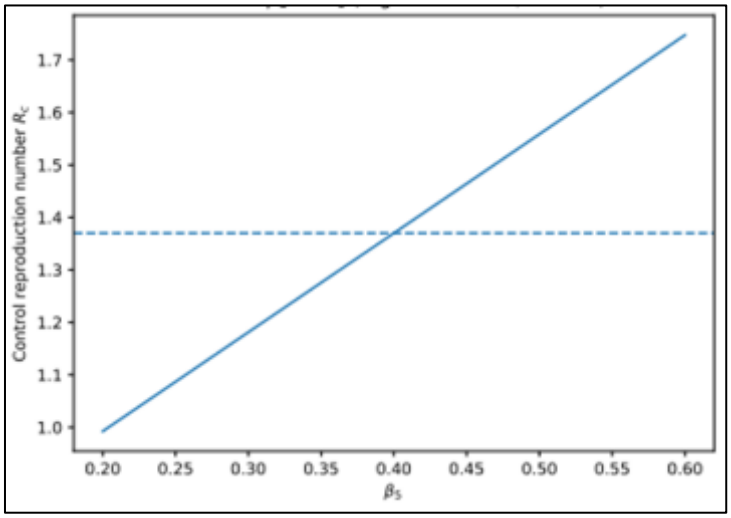

Figure 5 Effect of β_5 on R_c

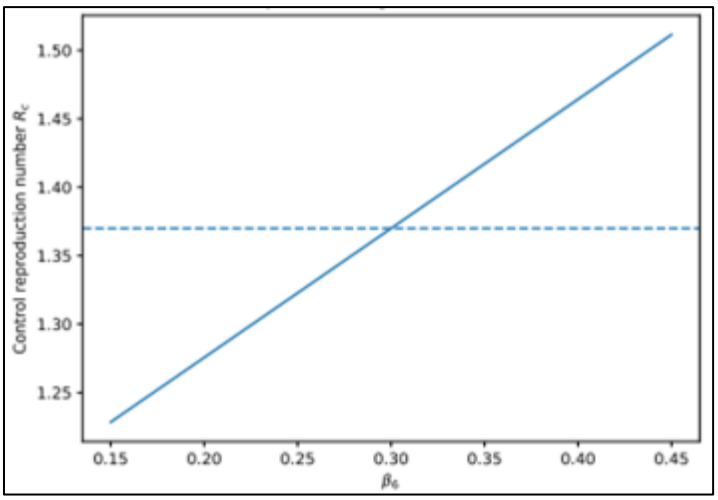

Figure 6 Effect of $\boldsymbol{\beta_6}$ on R_c

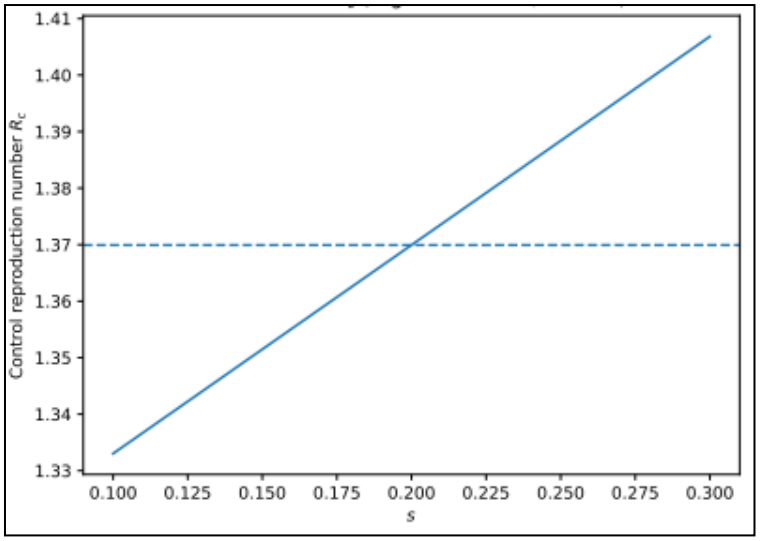

Figure 7 Effect of s on R_c

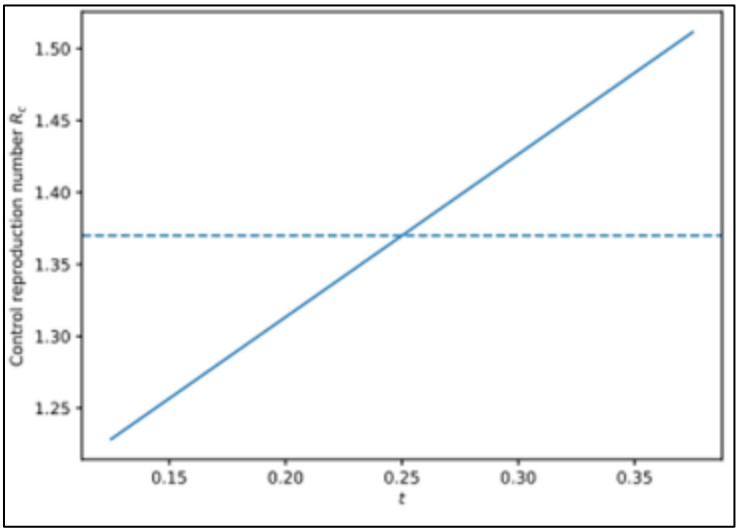

Figure 8 Effect of **t** on R_c

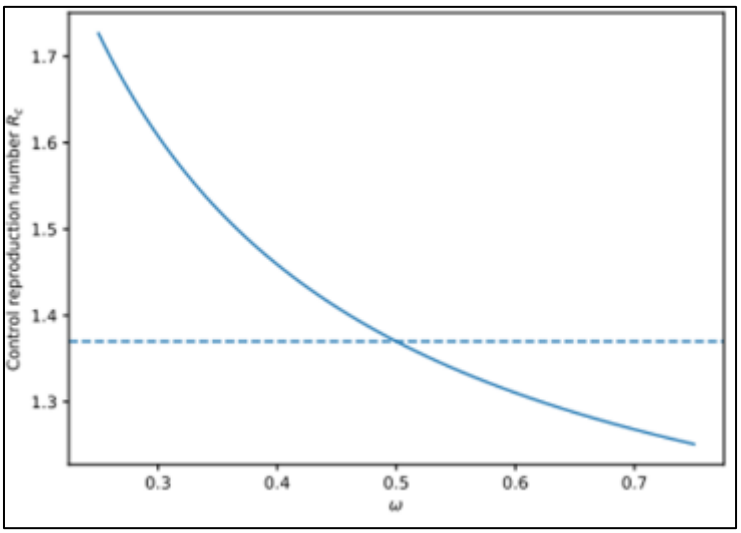

Figure 9 Effect of ω on R_c

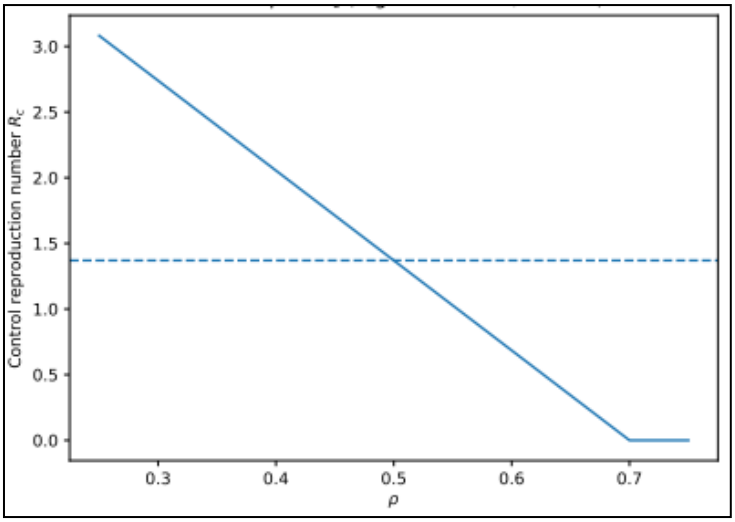

Figure 10 Effect of ρ on R_c

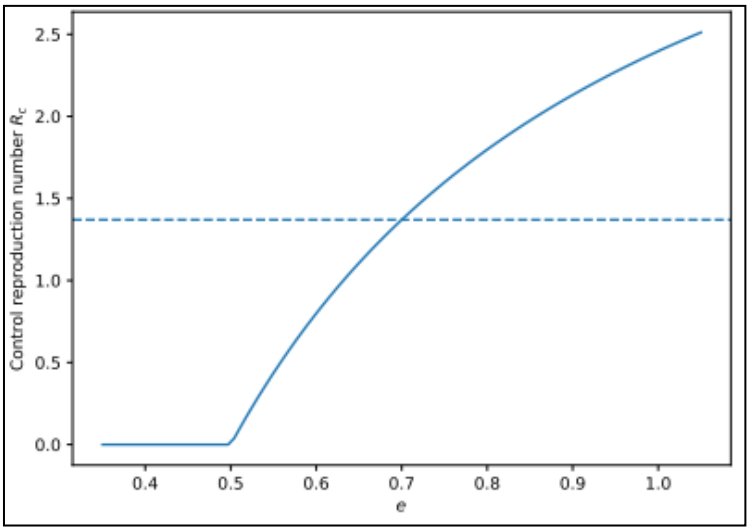

Figure 11 Effect of e on R_c

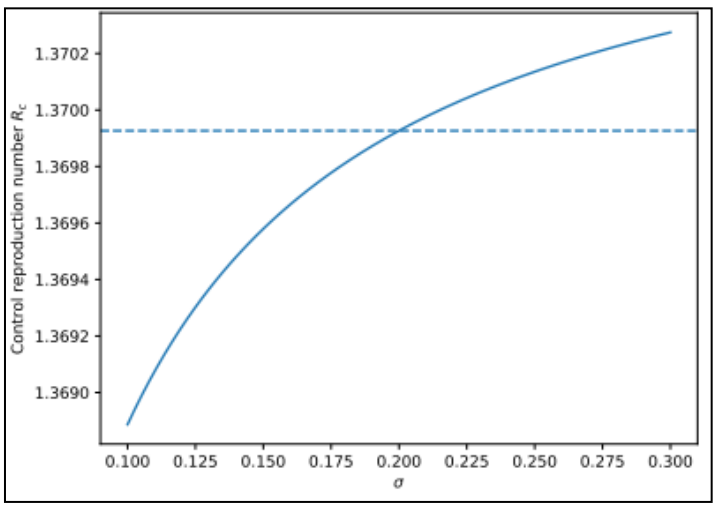

Figure 12 Effect of σ on R_c

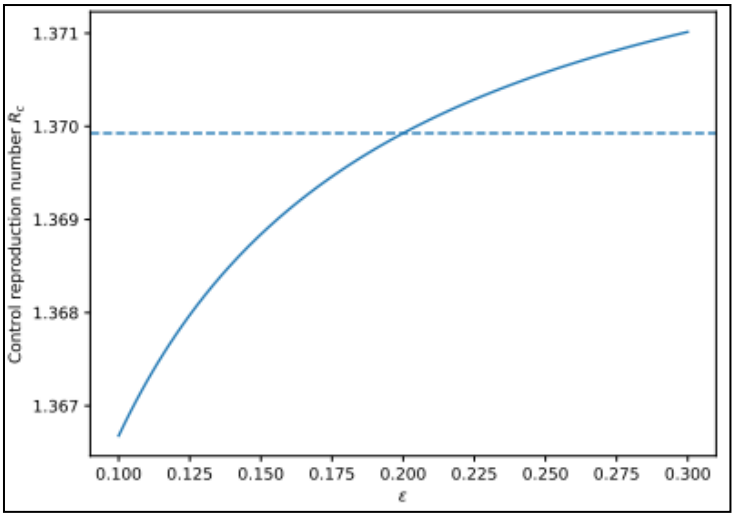

Figure 13 Effect of ε on R_c

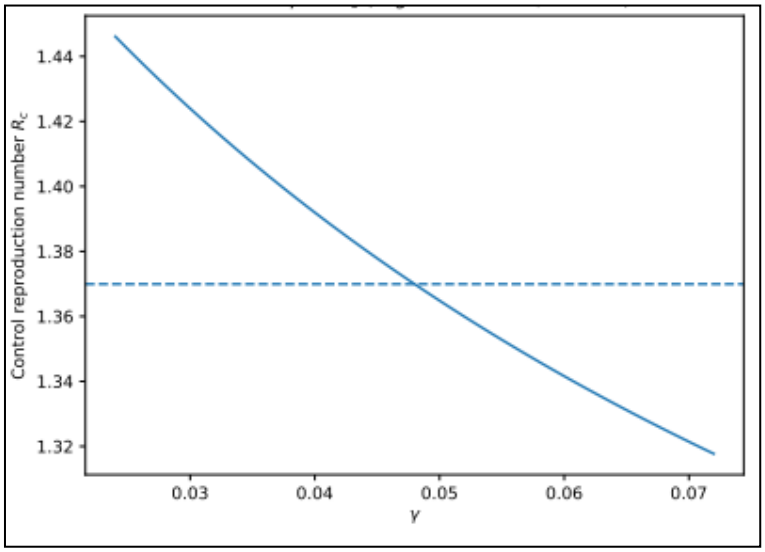

Figure 14 Effect of γ on R_c

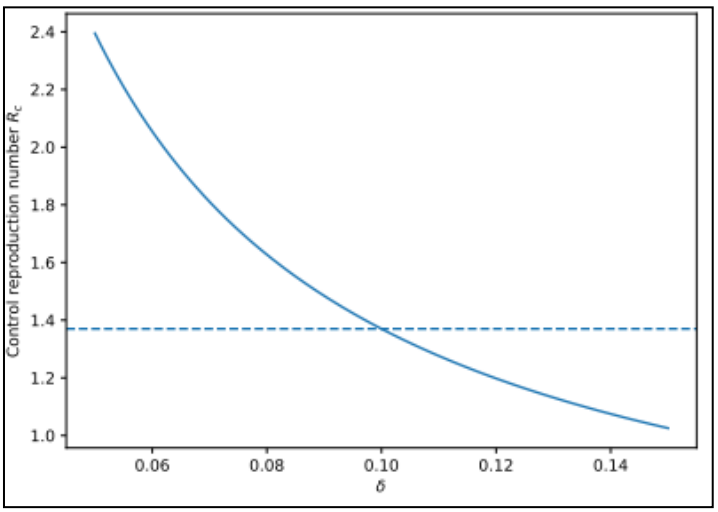

Figure 15 Effect of δ on R_c

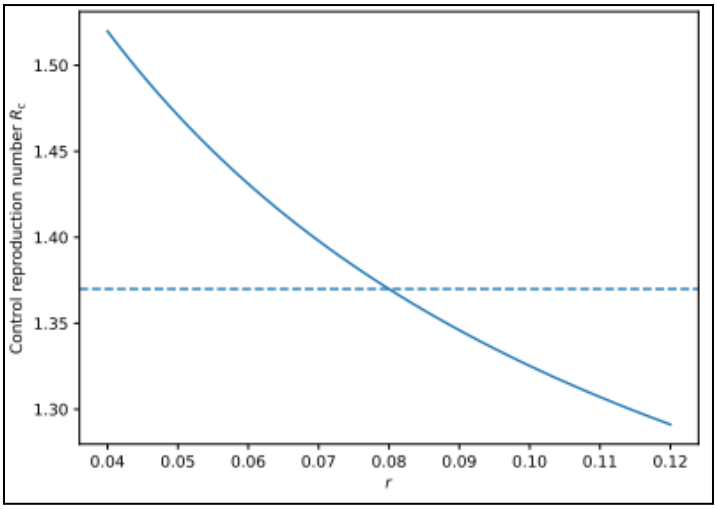

Figure 16 Effect of r on R_c

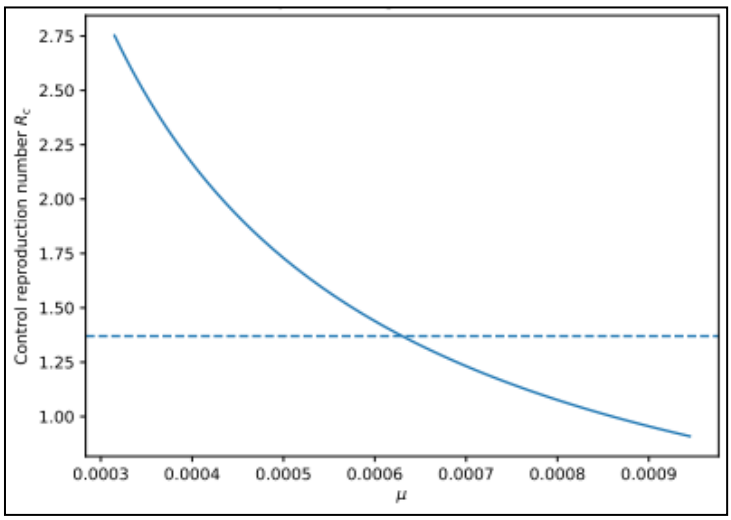

Figure 17 Effect of μ on R_c

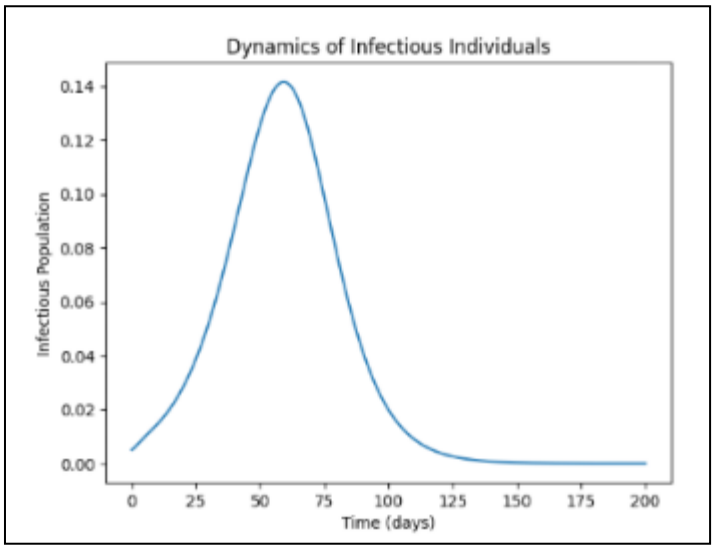

Figure 18 Graph of time evolution of infectious healthcare workers and infectious non-healthcare workers under baseline parameters

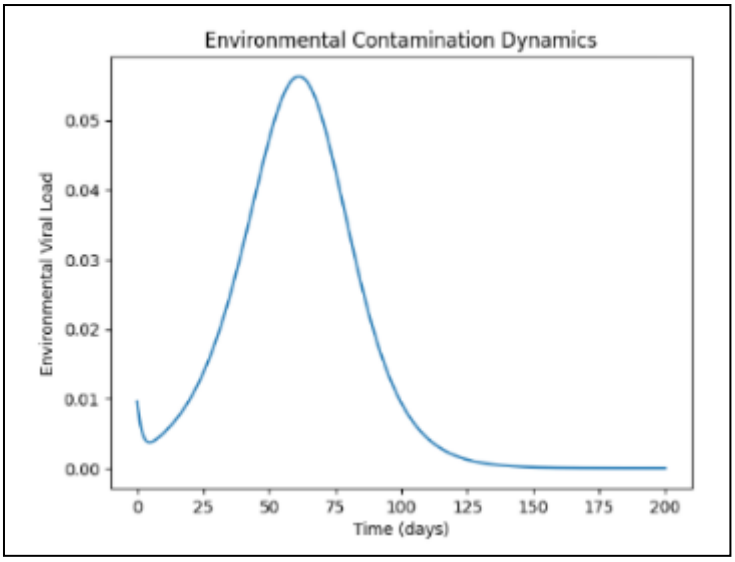

Figure 19 Graph of dynamics of environmental viral contamination over time

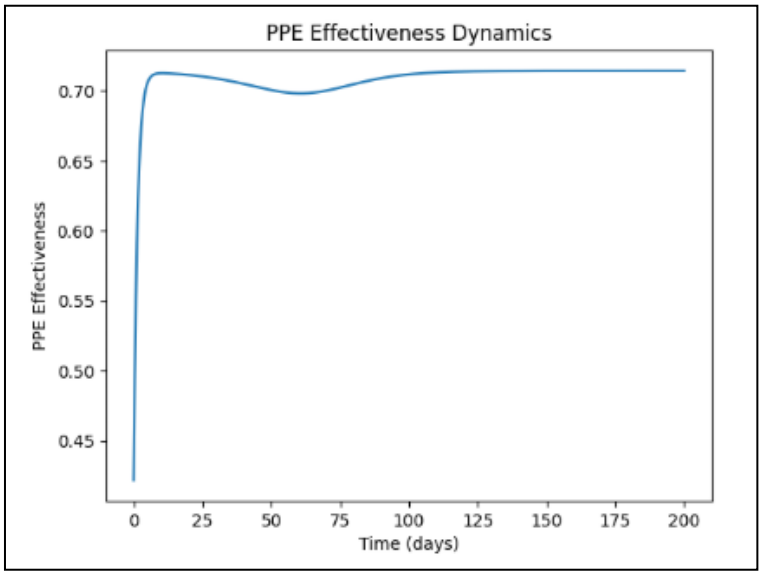

Figure 20 Graph of time evolution of PPE effectiveness under infection-induced depletion

6. Discussions

6.1. Effect of β_1 on R_c (Figure 3)

The graph shows a monotonic increase in R_c as β_1 increases, indicating that intensified contact among healthcare workers substantially elevates transmission. This reflects the critical role of occupational exposure within healthcare facilities.

6.2. Effect of β_3 on R_c (Figure 4)

An increase in β_3 leads to a steady rise in R_c, demonstrating that contaminated healthcare environments contribute meaningfully to infection risk, particularly when PPE effectiveness is limited.

6.3. Effect of β_5 on R_c (Figure 5)

This parameter exhibits the steepest positive slope among all graphs, confirming that community transmission is the dominant driver of COVID-19 spread. Small increases in β_5 result in pronounced increases in R_c.

6.4. Effect of β_6 on R_c (Figure 6)

The upward trend indicates that indirect transmission through contaminated community environments can sustain transmission even when direct contact rates are reduced.

6.5. Effect of s on R_c (Figure 7)

The graph shows a positive relationship between s and R_c, emphasizing that increased viral shedding by healthcare workers amplifies environmental contamination and secondary infections.

6.6. Effect of t on R_c (Figure 8)

Similarly, higher values of t elevate R_c, reinforcing the role of community-level contamination in prolonging outbreaks.

6.7. Effect of ω on R_c (Figure 9)

The negative slope demonstrates that improved cleaning and disinfection significantly suppress transmission by reducing indirect exposure pathways.

6.8. Effect of ρ on R_c (Figure 10)

This parameter shows one of the strongest negative effects on R_c . Increasing PPE availability markedly lowers transmission by protecting healthcare workers and interrupting hospital-based spread.

6.9. Effect of e on R_c (Figure 11)

An increase in e raises R_c, reflecting how PPE deterioration or misuse undermines protective effects and increases infection risk.

6.10. Effect of σ on R_c (Figure 12)

An increase in σ raises R_c by shortening the latent period, thereby accelerating the generation of new infectious individuals.

6.11. Effect of ε on R_c (Figure 13)

The positive slope mirrors that of σ, indicating that faster progression in the general population contributes to quicker epidemic growth.

6.12. Effect of γ on R_c (Figure 14)

The graph displays a decreasing trend, showing that faster recovery reduces the infectious period and lowers R_c.

6.13. Effect of δ on R_c (Figure 15)

Higher removal rates decrease R_c by shortening the duration of infectiousness in the community.

6.14. Effect of r on R_c (Figure 16)

Increasing isolation leads to a notable decline in R_c, highlighting the effectiveness of timely detection and isolation of infectious individuals.

6.15. Effect of μ on R_c (Figure 17)

The graph remains nearly flat, indicating that natural mortality has a negligible impact on COVID-19 transmission dynamics compared to epidemiological and control parameters.

6.16. Infectious Population Dynamics (Figure 18)

The temporal evolution of infectious healthcare workers and infectious non-healthcare workers shows a rapid initial increase, followed by convergence to endemic levels. This behavior is consistent with the analytical result that the endemic equilibrium is locally asymptotically stable when $R_c>1$. The larger peak observed among non-healthcare workers reflects the high sensitivity of R_c to the community transmission rate β_5, as identified in Table 4.

6.17. Environmental Contamination Dynamics (Figure 19)

The environmental viral load increases as a result of shedding from both infectious healthcare and non-healthcare workers and subsequently stabilizes due to environmental clearance. The persistence of environmental contamination highlights the role of indirect transmission pathways, consistent with the moderate positive sensitivity indices associated with s, t, β_3, and β_6.

6.18. PPE Effectiveness Dynamics (Figure 20)

The PPE effectiveness variable initially increases due to replenishment but declines as infection pressure rises, reflecting depletion and improper usage. The long-term behavior stabilizes at a lower level, emphasizing the strong negative sensitivity of R_c to the PPE replenishment rate ρ and the positive sensitivity to degradation rate e.

6.19. Policy Interpretation for Nigeria

The results of the extended COVID-19 transmission model highlight several policy-relevant insights for Nigeria. The sensitivity analysis indicates that the control reproduction number R_c is most strongly influenced by community transmission and exposure among healthcare workers, underscoring the need for sustained non-pharmaceutical interventions in public spaces and healthcare settings. In particular, the high sensitivity of R_c to the community transmission rate (β_5) suggests that policies targeting crowded environments such as public transport regulation, market spacing, and workplace infection-prevention protocols remain critical in controlling outbreaks.

The strong negative sensitivity associated with PPE replenishment (ρ) emphasizes the importance of maintaining reliable PPE supply chains for healthcare workers. Strengthening domestic PPE production, improving logistics to primary healthcare facilities, and enforcing proper PPE usage could substantially reduce transmission within healthcare settings. Similarly, the significant role of the recovery and isolation rates (γ and r) highlights the value of early case detection, rapid testing, and timely isolation, particularly in urban centers with high population density.

Environmental contamination parameters also exhibit meaningful influence on disease dynamics, indicating that routine disinfection of healthcare facilities and high-contact public environments should be integrated into outbreak response strategies. Given Nigeria's resource constraints, targeted environmental sanitation in hospitals, markets, and transportation hubs may offer cost-effective benefits.

Overall, the model suggests that an integrated control strategy combining community-level behavioral interventions, strengthened healthcare protection, adequate PPE provision, and environmental hygiene is essential for effective COVID-19 control in Nigeria. These findings provide quantitative support for reinforcing health system preparedness and prioritizing preventive investments during current and future infectious disease outbreaks.

7. Conclusion

An extended COVID-19 transmission model incorporating healthcare worker exposure, environmental contamination, and PPE dynamics has been developed and rigorously analyzed. The analytical results show that the disease-free equilibrium is globally stable when the control reproduction number is less than unity, while a unique endemic equilibrium exists and is locally asymptotically stable when transmission persists. Sensitivity analysis demonstrates that community transmission rates, PPE replenishment, recovery, and environmental clearance are the dominant drivers of the control reproduction number. Numerical simulations using Nigeria-specific data support the theoretical findings and highlight the importance of combined intervention strategies. Overall, the study emphasizes that effective COVID-19 control in Nigeria requires coordinated efforts to reduce community transmission, protecting healthcare workers, ensuring adequate PPE supply, and improving environmental hygiene. The modeling framework can be adapted to assess future outbreaks and inform preparedness strategies in similar low and middle income settings.

Recommendations

Effective COVID-19 control in Nigeria requires reducing community transmission through sustained public health measures, ensuring continuous PPE availability and proper usage among healthcare workers, and strengthening environmental sanitation in high-risk settings. Rapid testing, early isolation, and timely treatment should be prioritized to shorten infectious periods. Policymakers are encouraged to adopt model-based decision tools to guide resource allocation and improve preparedness for future outbreaks.

Future Work

Future studies may extend the present model by incorporating vaccination dynamics, waning immunity, and the emergence of new variants to capture long-term COVID-19 evolution. The model can also be refined using time-dependent parameters fitted to real-time epidemiological data from Nigeria. Further work may include optimal control analysis to evaluate cost-effective intervention strategies and stochastic modeling to assess uncertainty in transmission and reporting.

Compliance with ethical standards

Disclosure of conflict of interest

The authors declare that they have no known competing financial interests or personal relationships that could have appeared to influence the work reported in this paper.

Statement of ethical approval

This study is based on mathematical modeling and numerical simulations using parameter values obtained from published literature and publicly available reports. It does not involve human participants, animal subjects, or identifiable personal data. Therefore, ethical approval and informed consent were not required.

Data Availability

No new data were generated or analyzed in this study. All parameter values and supporting data were obtained from previously published studies and publicly accessible sources cited in the manuscript.

References

[1] Adebayo, A. O., Akinyemi, O. O., & Adebisi, Y. A. (2022). Modeling the transmission dynamics of COVID-19 in Nigeria. Infectious Disease Modelling, 7(1), 12–25. https://doi.org/10.1016/j.idm.2021.11.003

[2] Ajisegiri, W. S., Odusanya, O. O., & Joshi, R. (2020). COVID-19 outbreak situation in Nigeria and the need for effective engagement of community health workers for epidemic response. Global Biosecurity, 1(4), Article 69. https://doi.org/10.31646/gbio.69

[3] Chitnis, N., Hyman, J. M., & Cushing, J. M. (2008). Determining important parameters in the spread of malaria through the sensitivity analysis of a mathematical model. Bulletin of Mathematical Biology, 70(5), 1272–1296. https://doi.org/10.1007/s11538-008-9299-0

[4] Ferguson, N. M., Laydon, D., Nedjati-Gilani, G., Imai, N., Ainslie, K., Baguelin, M., … Ghani, A. C. (2020). Impact of non-pharmaceutical interventions (NPIs) to reduce COVID-19 mortality and healthcare demand(Report 9). Imperial College London. https://doi.org/10.25561/77482

[5] Kampf, G., Todt, D., Pfaender, S., & Steinmann, E. (2020). Persistence of coronaviruses on inanimate surfaces and their inactivation with biocidal agents. Journal of Hospital Infection, 104(3), 246–251. https://doi.org/10.1016/j.jhin.2020.01.022

[6] Kermack, W. O., & McKendrick, A. G. (1927). A contribution to the mathematical theory of epidemics. Proceedings of the Royal Society A, 115(772), 700–721. https://doi.org/10.1098/rspa.1927.0118

[7] Masandawa, B., Mukandavire, Z., & Garira, W. (2021). A COVID-19 mathematical model that incorporates healthcare workers and public health interventions. Computational and Mathematical Methods in Medicine, 2021, Article 5539216. https://doi.org/10.1155/2021/5539216

[8] Nigeria Centre for Disease Control. (2021). COVID-19 situation report. https://ncdc.gov.ng

[9] Nigeria Centre for Disease Control. (2022). National COVID-19 weekly epidemiological report. https://ncdc.gov.ng

[10] Ogunmodimu, O., Ojo, M. M., & Ogunniyi, A. (2022). Mathematical analysis of COVID-19 transmission dynamics in Nigeria. Journal of Applied Mathematics, 2022, Article 9987214. https://doi.org/10.1155/2022/9987214

[11] Shanafelt, T., Ripp, J., & Trockel, M. (2020). Understanding and addressing sources of anxiety among health care professionals during the COVID-19 pandemic. JAMA, 323(21), 2133–2134. https://doi.org/10.1001/jama.2020.5893

[12] van den Driessche, P., & Watmough, J. (2002). Reproduction numbers and sub-threshold endemic equilibria for compartmental models of disease transmission. Mathematical Biosciences, 180(1–2), 29–48. https://doi.org/10.1016/S0025-5564(02)00108-6

[13] van Doremalen, N., Bushmaker, T., Morris, D. H., et al. (2020). Aerosol and surface stability of SARS-CoV-2 as compared with SARS-CoV-1. New England Journal of Medicine, 382(16), 1564–1567. https://doi.org/10.1056/NEJMc2004973

[14] Wang, X., Tang, S., Cheke, R. A., & Tang, S. (2021). A stage-structured mosquito model incorporating environmental contamination. Mathematical Biosciences, 331, 108514. https://doi.org/10.1016/j.mbs.2020.108514

[15] World Health Organization. (2020). Transmission of SARS-CoV-2: Implications for infection prevention precautions. https://www.who.int

[16] World Health Organization. (2021). WHO COVID-19 global epidemiological update. https://www.who.int